Chapter 2
Properties of Amorphous Chalcogenides

2.1 Electrical Properties

Electrical properties of amorphous semiconductors have been described in various monographs, e.g. in [1]. As in the previous chapter, we shall only discuss the issues related to the subject of this book.

2.1.1 Pinning of the Fermi Level

In contrast to crystals, amorphous chalcogenides do not exhibit any significant change in conductivity upon doping. This fact was first established by Kolomiets [2] and is usually explained by the Mott rule (cf. Sect. 1.5.1).

The temperature dependence of the dark conductivity of chalcogenide glasses follows an exponential dependence (Fig. 2.1) with the activation energy close to $E_g/2$ implying (i) intrinsic-like semiconducting behaviour and/or (ii) a large concentration of gap states that fix the Fermi level at midgap position [1]. This situation is usually called pinning of the Fermi level. Even when impurities are added in concentrations that do change the optical gap, the Fermi level remains pinned close to the centre of the gap. Similar results, i.e. the location of the Fermi level remaining in the middle of the gap independent of doping, have been reported for the amorphous phase of phase-change materials [3].

While under certain circumstances the chalcogenide glasses *can* be doped, the concentration of impurities (usually Bi) is usually larger than 10% [4]; this process is usually referred to as modification.

2.1.2 P-Type Conductivity

With just a few exceptions, amorphous chalcogenides are *p*-type semiconductors. The reason for this is not clear [6]. One of the explanations offered was that the

A. V. Kolobov and J. Tominaga, *Chalcogenides*, Springer Series in Materials Science 164, DOI: 10.1007/978-3-642-28705-3_2,

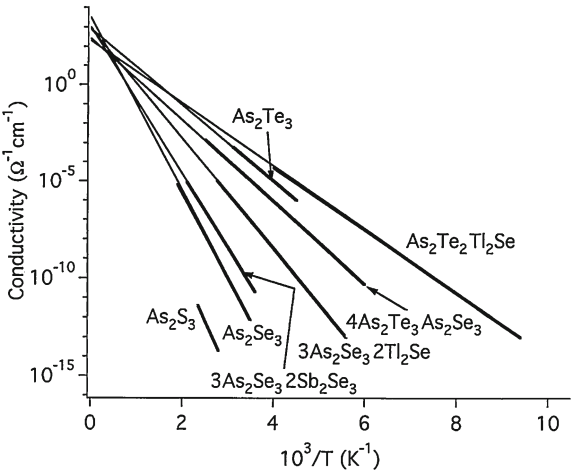

Fig. 2.1 Temperature dependence of dark conductivity of typical chalcogenide glasses (Reprinted with permission by Oxford University Press from Mott and Davis [5])

fluctuations in the conduction band tail are larger than those in the valence band, which leads to stronger localisation of electrons [6]. For crystalline GeTe that is an end point for the quasibinary $Ge_2Sb_2Te_5$-Sb_2Te_3 phase-change alloys it was argued that *p*-type conductivity is due to presence of vacancies on the Ge sublattice [7].

2.1.3 Hall Effect Anomaly

The conductivity type (*p*-type) of chacogenide glasses is determined by thermo-conductivity measurements using the Seebeck effect. Application of Hall effect measurements usually yields an opposite (n-) sign for the conductivity type. This phenomenon is referred to as the anomalous Hall effect and has been interpreted in terms of small polarons [8] or three-site interactions [9]. The Hall effect anomaly has also been observed for amorphous phase-change materials [10].

2.1.4 Phase-Change Materials

Phase-change materials of which $Ge_2Sb_2Te_5$ is a prototypical example, crystallise at temperatures around 160 °C. Crystallisation results in a drastic increase in their conductivity [11, 12] as illustrated by Fig. 2.2.

The temperature dependence of the dark conductivity of $Ge_2Sb_2Te_5$ in the amorphous and crystalline phases is shown in Fig. 2.3 [13]. In addition to the fact that conductivity in the crystalline phase is several orders of magnitude higher than in the amorphous phase, one can also see that while the amorphous and fcc phases are semiconducting (the conductivity increases with temperature), the hexagonal phase is believed to be metallic.

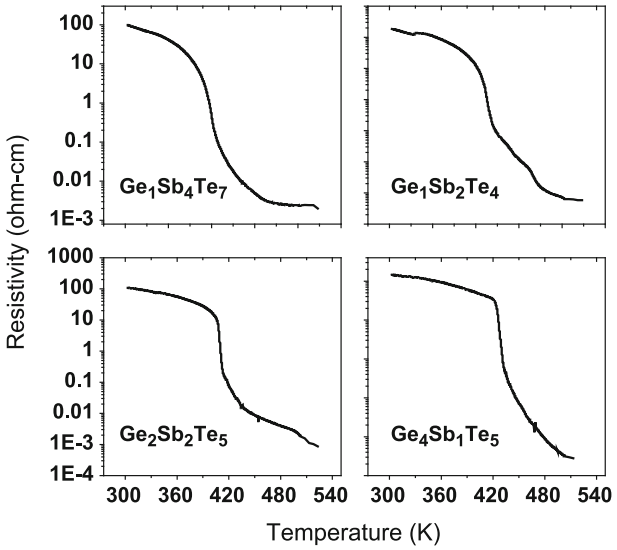

Fig. 2.2 Drastic change in dark conductivity accompanying the crystallisation of Ge-Se-Te alloys. Reprinted from Morales-Sánchez et al. [12] with permission from Elsevier

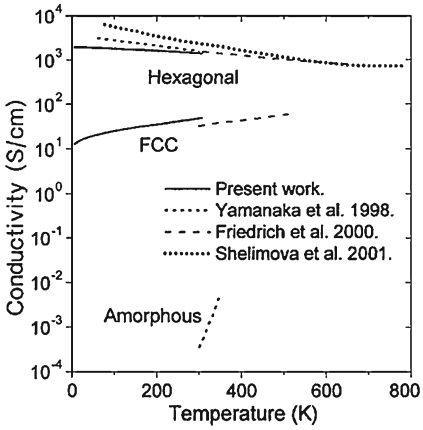

Fig. 2.3 Temperature dependence of the electrical dark conductivity of $Ge_2Sb_2Te_5$ in amorphous and crystalline (both the stable hexagonal and metastable face-centered cubic) phases. Reprinted with permission from Lee et al. [13]. Copyright 2005 by the American Institute of Physics (The label 'present work' in the figure refers to the cited work)

Semiconductors of Metals?

It is interesting to note that there is no general consensus on the conductivity type of the crystalline phases of GST. Thus, Lee et al. [13] proposed that the hexagonal phase of $Ge_2Sb_2Te_5$ is a narrow-gap degenerate semiconductor, where the Fermi level is within the valence band while based on the sign of the slope of temperature dependence of conductivity Wuttig argued that this phase is metallic [11, 14].

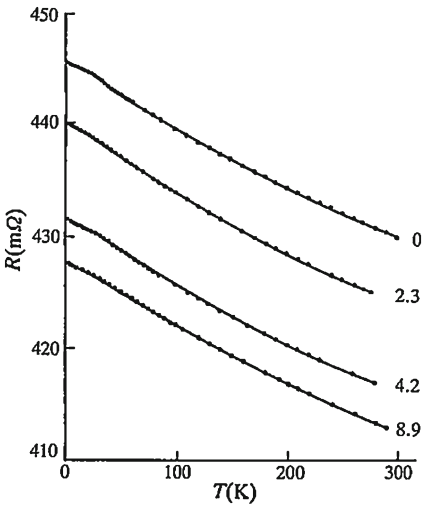

Fig. 2.4 Resistance of amorphous $Cu_{57}Zn_{43}$ as a function of temperature (with and without a magnetic field shown in Tesla). Reprinted from Fritsch et al. [15] with permission from IOP Publishing Ltd.

The fcc phase is generally described as a degenerate p-type semiconductor with a hole concentration of ca. $10^{20}\,\mathrm{cm}^{-3}$ and a mobility of ca. $1\,\mathrm{cm}^2/\mathrm{V\,s}$ although there are some results suggesting that the fcc phase is nondegenerate. At the same time, it should be noted that the experimentally observed variation in the temperature dependence of the conductivity is rather weak and similar to those observed in amorphous or 'dirty' metals [16] as illustrated in Fig. 2.4. The latter also refers to the liquid phase of $Ge_2Sb_2Te_5$.

It is interesting to note that the dielectric constant $\epsilon_1(\omega)$ of most phase-change materials (except GeTe) remains positive at all frequencies [17], which, again, is typical of 'dirty' metals where the plasma oscillations are overdamped [18].

2.1.5 Chalcogenides as Topological Insulators

Recently, a new class of materials called topological insulators [19] has been intensely investigated. Topological insulators are materials with a bulk insulating gap and protected conducting surface states arising from a combination of spin–orbit interactions and time-reversal symmetry which limits possible candidates to heavy elements and rather narrow bandgap materials. It was speculated that topological insulators may be promising materials for quantum computing [20]. So far, topological insulator behaviour has been observed in $Bi_{1-x}Sb_x$ alloys and some A_2B_3 crystals including Sb_2Te_3 [21–23].

It was also predicted that topological properties of $Ge_2Sb_2Te_5$ strongly depend on the stacking sequence along the ⟨111⟩ direction (cf. Sect. 8.1.2). Thus, $Ge_2Sb_2Te_5$ with the Petrov stacking sequence along the ⟨111⟩ direction was predicted be a

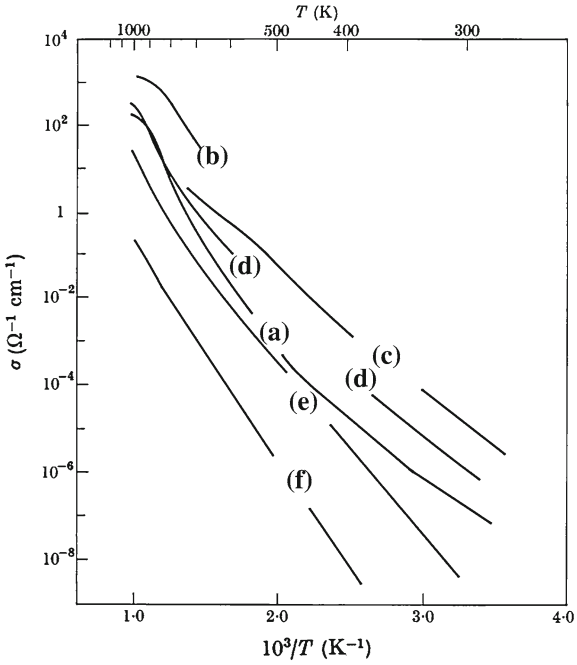

Fig. 2.5 Temperature variation of conductivity for several chalcogenide glasses in the solid and liquid states (*a*) $As_{30}Te_{48}Si_{12}Ge_{10}$; (*b*) As_2Te_3; (*c*) $As_2S_3Tl_2Te$; (*d*) As_2SeTe_2; (*e*) As_2Se_2Te; (*f*) As_2Se_3 (Reprinted with permission by Oxford University Press from Mott and Davis [5])

topological insulator while the Kooi sequence should exhibit surface-like conducting states [24]. A further prediction is that pressure modifies topological insulator properties of phase-change alloys. In particular, it was shown using DFT simulations that hexagonal $Ge_2Sb_2Te_5$ with the Kooi layer sequence transforms from a normal semiconductor to a topological insulator at a hydrostatic pressure of ca. 2.6 GPa, and reverts to a semiconductor at ca. 4.5 GPa, while $Ge_2Sb_2Te_5$ with Petrov sequence maintains a topological insulator state from zero pressure to 2.3 GPa.

2.1.6 Liquid Chalcogenides

Upon melting, chalcogenide glasses tend to preserve the semiconducting behaviour as illustrated by Fig. 2.5 for typical chalcogenide glasses [1]. This behaviour suggests that melting of chalcogenides proceeds without destruction of the covalent backbone of the structure.

A similar conclusion was made for liquid $Ge_2Sb_2Te_5$ based on the sign of the temperature dependence of conductivity (Fig. 2.6) [25] although the observed temperature dependence of conductivity was rather weak.

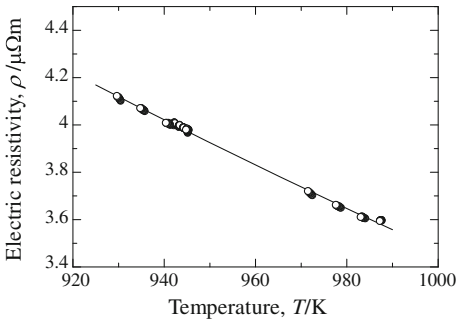

Fig. 2.6 Temperature dependence of conductivity of liquid $Ge_2Sb_2Te_5$ alloy. Reprinted with permission by Japan Society of Applied Physics from Endo et al. [25]

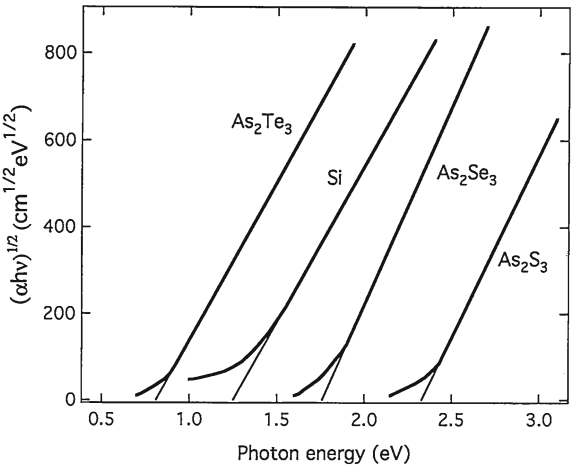

Fig. 2.7 Spectral dependence of optical absorption above the absorption edge for typical amorphous semiconductors (Reprinted with permission by Oxford University Press from Mott and Davis [5])

2.2 Optical Absorption

2.2.1 Interband Absorption

Figure 2.7 shows spectral dependencies of absorption coefficients for typical amorphous semiconductors [1]. As can be seen, this dependence can be described by the relation

$$\alpha h\nu = B(h\nu - E_0)^2 \tag{2.1}$$

This relationship is often called the Tauc law. The coefficient B is of the order of 10^5 $cm^{-1}eV^{-1}$. This kind of spectral behaviour is fairly easy to understand assuming parabolic dependencies for the density of valence and conduction band states.

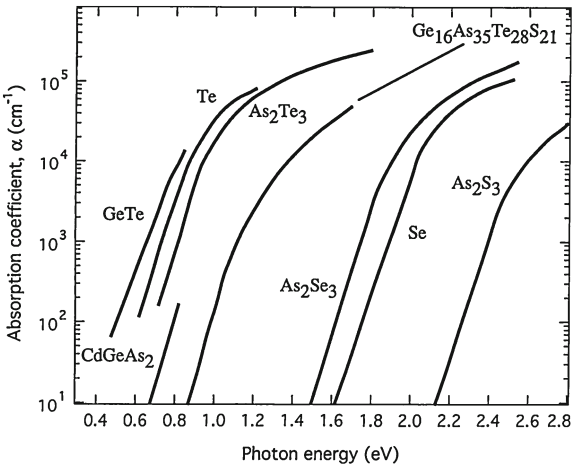

Fig. 2.8 Exponential absorption edge in amorphous semiconductors at room temperature (Reprinted with permission by Oxford University Press from Mott and Davis [5])

2.2.2 Absorption Edge (the Urbach Rule)

The presence of sharp band edges in crystals results in a sharp increase in the absorption coefficient when the photon energies exceed the optical gap. In amorphous chalcogenides, the presence of energy band tails results in significant absorption even at photon energies below the optical gap. Typical spectral dependencies for energies at the absorption edge [1] are shown in Fig. 2.8.

It can be seen that the absorption below the edge is described by an exponential dependence:

$$\alpha = \alpha_0 \exp[-\gamma(E_0 - h\nu)/kT] \tag{2.2}$$

which is usually called the Urbach rule. Here γ is a material constant and T is absolute temperature down to a critical value T_0 and equals T_0 for lower temperatures. It is interesting to note that, despite rather large differences in the bandgap, the slope of the Urbach edge, γ, is almost the same for various materials, typically ca. 50 meV. This constancy weakens a possible explanation that the Urbach rule results from the exponential distribution of the tail states that should vary from one material to another. Several possible mechanisms have been proposed [26–29]. In [27] it was suggested that the Urbach edge arises from an electric-field broadening of the exciton line. Although usually the exciton line has a Gaussian shape, in the presence of a uniform electric field it was shown to become exponential over a wide range of energies [27]. The responsible electric fields may arise, for example, from static spatial fluctuations, density variations and presence of charged defects.

An electric field was also considered to cause exponential absorption dependence through interaction of a bound exciton with lattice vibrations [26] leading to electric-field broadening of the absorption edge similar to the Franz–Keldysh effect.

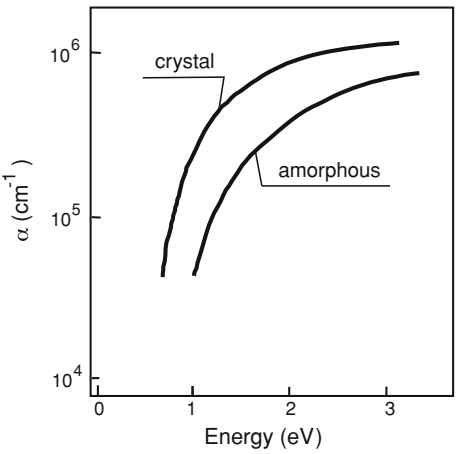

Fig. 2.9 Spectral dependence of absorption coefficients α of as-deposited amorphous and crystalline $Ge_2Sb_2Te_5$

Strong electron–phonon interaction was argued to be an alternative reason for the exponential dependence of the absorption coefficient [28, 30]. Within this approach, the slope of the Urbach edge ($u = kT/\gamma$) and absorption at larger energies were shown to be related through the following equation:

$$u = (4\alpha_0 E_0/3B)^{1/2} \tag{2.3}$$

where α_0 is the absorption coefficient at the bandgap energy E_0 and B is a parameter used for the interband absorption coefficient.

To summarise this discussion, it should be noted that such a variety of "successful" approaches to explain the exponential dependence is at the same time an indication that the question of its origin still remains open.

2.2.3 Phase-Change Materials

The spectral dependencies of optical constants for the prototypical phase-change material $Ge_2Sb_2Te_5$ in as-deposited amorphous and crystalline phases have been studied by various authors [13, 31–34] and there is a very good agreement between the results obtained by different groups. Fig. 2.9 shows generic absorption spectra for the amorphous and crystalline phases. The optical gaps have been determined as 0.7 eV for as-deposited amorphous $Ge_2Sb_2Te_5$ and 0.5 eV for the crystalline phase and the Urbach energy was found to be 80 meV for $Ge_2Sb_2Te_5$ [13], the latter value is slightly higher than that for chalcogenide glasses despite a smaller bandgap.

Since in optical devices using phase-change materials a change in optical reflectivity is employed, it is occasionally more convenient to use optical constants n and k to characterise the amorphous and crystalline phases [35]. The corresponding plots

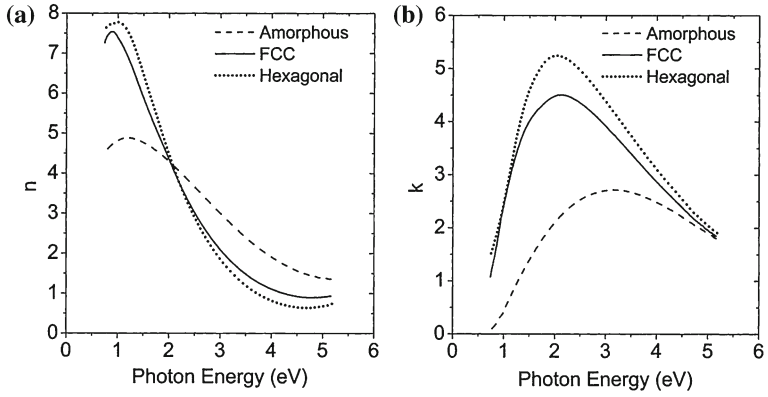

Fig. 2.10 Optical constants n (**a**) and k (**b**) of amorphous, fcc and hexagonal phases of $Ge_2Sb_2Te_5$, after Lee and Bishop [35]. Reprinted with permission from Springer

are shown in Fig. 2.10. It is interesting to note that computer simulations of the optical properties of Ge-Sb-Te phase-change alloys started in 1997 [36] and produced the results that are in very good agreement with experiment.

2.3 Photoexcitation and Recombination

Illumination of semiconductors with light having photon energies exceeding that of the optical gap generates electron–hole pairs. The photoexcited charge carriers of different signs can then either separate, giving rise to photoconductivity, or recombine, either radiatively (photoluminescence) or nonradiatively. Non-radiative recombination can, in principle, transfer the material into a state different from the one prior to irradiation. Such a possibility is especially likely in amorphous semiconductors, where the structure is more flexible than in the corresponding crystals and where structural disorder leads to localisation of charge carriers.

The recombination is called geminate if the very same electron and hole that were created recombine. This happens when the carriers do not drift apart, that is, at low temperatures, low mobilities or low light intensities. Below we briefly discuss specific features of photoluminescence in chalcogenide glasses.

2.3.1 Photoluminescence

Photoluminescence and excitation spectra for typical chalcogenide glasses, a-Se, As_2S_3 and As_2Se_3 [37, 38], are shown in Fig. 2.11. The main feature is a broad band centred at about half the bandgap energy. Interestingly, similar features are observed in crystalline chalcogenides [39].

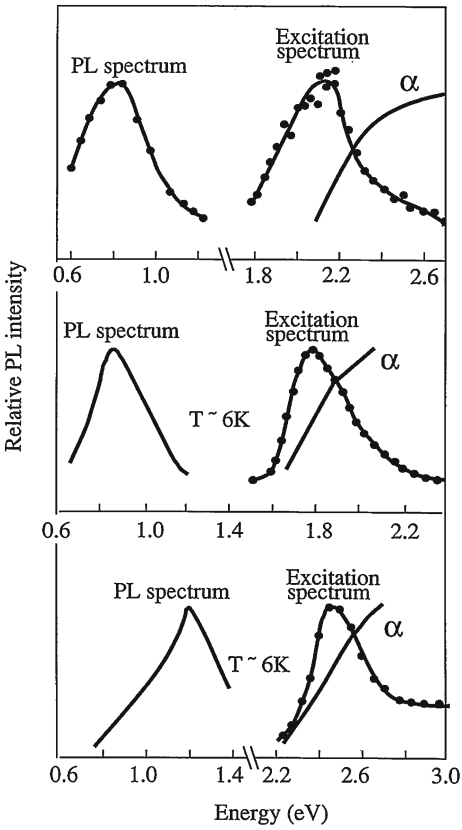

Fig. 2.11 *Top* Photoluminescence spectra, excitation spectra and absorption spectra for a-Se (reprinted from Street et al. [37] with permission from Taylor and Francis). *Middle and bottom* Photoluminescence spectra, excitation spectra and absorption spectra for As_2Se_3, and As_2S_3. Reprinted with permission from Bishop and Mitchell [38]. Copyright 1973 by the American Physical Society

The large difference between the luminescence energy and the bandgap implies that recombination occurs through deep states. Early models suggested that recombination takes place from the conduction band into deep states or between the tail states. These models tacitly assumed that the electron–phonon interaction is weak. It seems more likely, however, that electron–phonon coupling plays an important role in the recombination process [39].

The essence of this approach is illustrated by the coordination-coordinate diagram shown in Fig. 2.12. The adiabatic potentials are given by

$$E_1(q) = Aq^2 \tag{2.4}$$

$$E_2(q) = E_0 + Aq^2 - Bq \tag{2.5}$$

for the ground and excited states, respectively; A is related to the vibrational frequency ω through the equation $A = M\omega^2/2$, where M is the effective mass and B is the measure of electron–phonon coupling. The meaning of other parameters is

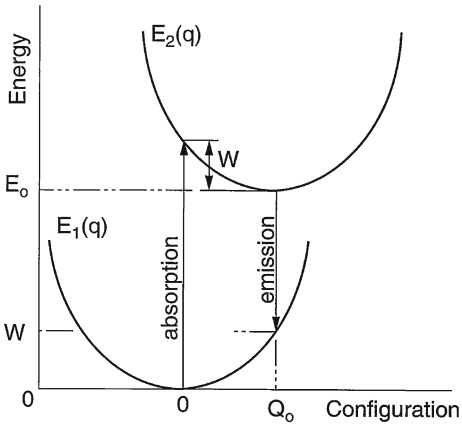

Fig. 2.12 Configuration-coordinate diagram illustrating optical absorption and emission in a system with strong electron–phonon coupling

obvious from the figure. It can be easily shown [39] that within this approximation the photoluminescence line shape is Gaussian and shifted by $2W$ to lower energies compared to the absorption edge.

The excitation spectrum measures the dependence of luminescence intensity on the excitation energy. In most chalcogenides this spectrum is presented by a broad peak close to the bandgap. The excitation mechanism is band-to-band absorption followed by the capture of carriers by recombination centres. A decrease in the intensity at lower energies is due to incomplete absorption whereas a decrease at higher energies most likely arises from the energy dependence of the quantum efficiency [39].

No data are available in the literature on photoluminescence in phase-change materials.

2.3.2 Photo-Induced Metastability

The phenomena described above do not change the structural state of the material. At the same time, being intrinsically metastable, amorphous semiconductors can be easily transferred between different metastable states by external stimuli such as light [40–42]. We would like to mention here that *meta*stable does not mean *un*stable. Thus diamonds are a metastable form of carbon with the stable phase being graphite. Despite this metastability diamonds are stable over a very large temperature and pressure range. Another example of a stable metastable state is stained-glass windows of medieval churches that remained essentially unchanged for centuries. Various aspects of metastability of chalcogenide glasses are described in detail in Chaps. 4 and 6 and structural transformations in phase-change materials are the subject of Chaps. 10 and 11.

References

1. N.F. Mott, E.A. Davis, *Electronic Processes in Non-Crystalline Materials*, 2nd edn. (Clarendon Press, Oxford, 1979)
2. B.T. Kolomiets, Phys. Stat. Sol. (b) **7**, 359 (1964)
3. S. Caravati, M. Bernasconi, T. Kühne, M. Krack, M. Parrinello, J. Phys. Condens. Matter **21**, 255501 (2009)
4. R. Rajesh, J. Philip, J. Appl. Phys. **93**, 9737 (2003)
5. N.F. Mott, E.A. Davis, *Electronic Properties of Non-Crystalline Materials*, 2nd edn. (Oxford University Press, Oxford, 1979)
6. A.V. Kolobov, J. Non-Cryst. Solids **198**, 728 (1996)
7. A.H. Edwards, A.C. Pineda, P.A. Schultz, M.G. Martin, A.P. Thompson, H.P. Hjalmarson, J. Phys. Condens. Matter **17**, L329 (2005)
8. D. Emin, Philos. Mag. **35**, 1189 (1977)
9. S.R. Elliott, *Physics of Amorphous Materials*, 2nd edn. (Longman, London, 1984)
10. S.A. Baily, D. Emin, H. Li, Solid State Commun. **139**, 161 (2006)
11. I. Friedrich, V. Weidenhof, W. Njoroge, P. Franz, M. Wuttig, J. Appl. Phys. **87**, 4130 (2000)
12. E. Morales-Sánchez, E.F. Prokhorov, J. Gonzalez-Hernandez, A. Mendoza-Galvan, Thin Solid Films **471**, 243 (2005)
13. B.S. Lee, J.R. Abelson, S.G. Bishop, D.H. Kang, B.K. Cheong, K.B. Kim, J. Appl. Phys. **97**, 093509 (2005)
14. T. Siegrist, P. Jost, H. Volker, M. Woda, P. Merkelbach, C. Schlockermann, M. Wuttig, Nature Mater. **10**, 202 (2011)
15. G. Fritsch et al., J. Phys. F Metal Phys. **12**, 2965 (1982)
16. N.F. Mott, *Conduction in Non-Crystalline Materials* (Clarendon Press, Oxford, 1987)
17. K. Shportko, S. Kremers, M. Woda, D. Lencer, J. Robertson, M. Wuttig, Nature Mater. **7**, 653 (2008)
18. R. Kiebooms, R. Menon, K. Lee, in *Handbook of Advanced Electronic and Photonic Materials and Devices*, vol. 8, ed. by H.S. Nalwa (Academic Press, San Diego, 2001), p. 1
19. M.Z. Hasan, C.L. Kane, Rev. Mod. Phys. **82**, 3045 (2010)
20. J. Moore, Nature Phys. **5**, 378 (2009)
21. H. Zhang, C.X. Liu, X.L. Qi, X. Dai, Z. Fang, S.C. Zhang, Nature Phys. **5**, 438 (2009)
22. G. Wang, X. Zhu, J. Wen, X. Chen, K. He, L. Wang, X. Ma, Y. Liu, X. Dai, Z. Fang, J. Jia, Q. Xue, Nano Res. **3**, 874 (2010)
23. D. Hsieh, Y. Xia, D. Qian, L. Wray, F. Meier, J.H. Dil, J. Osterwalder, L. Patthey, A.V. Fedorov, H. Lin, A. Bansil, D. Grauer, Y.S. Hor, R.J. Cava, M.Z. Hasan, Phys. Rev. Lett. **103**, 146401 (2009)
24. J. Kim, J. Kim, S.H. Jhi, Phys. Rev. B **82**, 201312 (2010)
25. R. Endo, S. Maeda, Y. Jinnai, R. Lan, M. Kuwahara, Y. Kobayashi, M. Susa, Jpn. J. Appl. Phys. **49**, 5802 (2010)
26. Y. Toyozawa, Progr. Theor. Phys. **22**, 455 (1959)
27. J. Dow, Phys. Rev. B **5**, 594 (1972)
28. A.V. Kolobov, O.V. Konstantinov, Philos. Mag. B **40**, 475 (1979)
29. B.L. Gelmont, V.I. Perel, I.N. Yassievich, Fiz. Tverd. Tela **25**, 727 (1983)
30. A.V. Kolobov, O.V. Konstantinov, Philos. Mag. B **47**, 1 (1983)
31. D.V. Tsu, J. Vac. Sci. Technol. A **17**, 1854 (1999)
32. S.Y. Kim, S.J. Kim, H. Seo, M.R. Kim, Jpn. J. Appl. Phys. **38**, 1713 (1999)
33. E. Garcia-Garcia, A. Mendoza-Galvan, Y. Vorobiev, E. Morales-Sanchez, J. Gonzalez-Hernández, G. Martinez, B.S. Chao, J. Vac. Sci. Technol. A **17**, 1805 (1999)
34. A. Pirovano, A.L. Lacaita, A. Benvenuti, F. Pellizzer, R. Bez, IEEE T. Electron Dev. **51**, 452 (2004)
35. B.S. Lee, S.G. Bishop, in *Phase Change Materials: Science and Applications*, ed. by S. Raoux, M. Wuttig (Springer, Berlin, 2009), p. 175

36. S. Ogawa, S. Yamanaka, Y. Ueshima, I. Morimoto, in *9th Symposium on Phase Change Optical Information Storage* (*PCOS'97*), Numadu, 1997, p. 50
37. R.A. Street, T.M. Searle, I.G. Austin, Philos. Mag. **29**, 1157 (1974)
38. S.G. Bishop, D.L. Mitchell, Phys. Rev. B **8**, 5696 (1973)
39. R.A. Street, Adv. Phys. **25**, 397 (1976)
40. K. Shimakawa, A.V. Kolobov, S.R. Elliott, Adv. Phys. **44**, 475 (1995)
41. N. Itoh, M. Stoneham, *Materials Modification by Electronic Excitation* (Cambridge University Press, Cambridge, 2001)
42. A.V. Kolobov (ed.), *Photo-Induced Metastability in Amorphous Semiconductors* (Wiley-VCH, Winheim, 2003)

http://www.springer.com/978-3-642-28704-6

Chalcogenides
Metastability and Phase Change Phenomena
Kolobov, A.V.; Tominaga, J.
2012, XVI, 284 p., Hardcover
ISBN: 978-3-642-28704-6